Theoretical Background. The chemical reaction parameters can be obtained from the following formula [1-3]:

$$IP=E_{+}-E_{0} \quad (1)$$

$$EA=E_{0}-E_{-} \quad (2)$$

$$h=\frac{IP-EA}{2} \quad (3)$$

$$W=\frac{(IP+EA)^{2}}{4(IP-EA)} \quad (4)$$

$$W^{+}=\frac{(IP+3EA)^{2}}{16(IP-EA)} \quad (5)$$

Where E_{+} is the energy of the cation, and E_{-} is the energy of the anion, and E_{0} is the energy calculated from the optimized structure of the neutral molecule.

The intramolecular charge transfer characteristics can be obtained from the following formula [4-6]:

$$D_{ct}=\sqrt{D_{X}^{2}+D_{Y}^{2}+D_{Z}^{2}} \quad (6)$$

$$\Delta q=\int \rho_{+}(r)dr=\int \rho_{-}(r)dr \quad (7)$$

Where D_{ct} is the charge transfer distance, and D_X, D_Y, D_Z represent the distance in three different directions; the overlap condition, $\rho_{+}(r)$ and $\rho_{-}(r)$ are increment and depletion of the density.

The essence of the nonlinear optics (NLO) property is to describe the response of a system in an applied electric field, which in turn affects intramolecular charge delocalization based upon asymmetric polarization caused by the donor and receptor segments in π-conjugated molecules, The molecular polarizability is calculated by Taylor expansion of energy E to uniform external electric field F:

$$\begin{aligned} E(F) &= E(0)+\frac{\partial E}{\partial F}\bigg|_{F=0}F+\frac{1}{2}\frac{\partial^{2}E}{\partial F^{2}}\bigg|_{F=0}F^{2}+\frac{1}{6}\frac{\partial^{3}E}{\partial F^{3}}\bigg|_{F=0}F^{3}+\ldots \\ &= E(0)-\mu_{0}F-\frac{1}{2}\alpha F^{2}-\frac{1}{6}\beta F^{3}-\ldots \end{aligned} \quad (8)$$

$$\alpha = -\frac{\partial^2 E}{\partial F^2}\Big|_{F=0} \qquad (9)$$

$$\beta = -\frac{\partial^3 E}{\partial F^3}\Big|_{F=0} \qquad (10)$$

μ_0 is the vector of the molecule's permanent dipole moment (the dipole moment in the absence of an external field). α is the molecular polarizability, also known as the linear optical coefficient. β is the first hyperpolarizability, or the NLO coefficient of the molecule. The polarizability is calculated by the following formula [7]:

$$\alpha = (\alpha_{XX} + \alpha_{YY} + \alpha_{ZZ})/3 \qquad (11)$$

Where α_{xx}, α_{yy}, and α_{zz} denote the tensor components of polarizability, respectively. The tensor of the β represents a result of the third derivative of the energy, which is written as [8]:

$$\beta_{tot} = \sqrt{(\beta_{xxx} + \beta_{xyy} + \beta_{xzz})^2 + (\beta_{yyy} + \beta_{xxy} + \beta_{yzz})^2 + (\beta_{zzz} + \beta_{xxz} + \beta_{yyz})^2} \qquad (12)$$

The electron injection driving force and electron regeneration driving force are obtained from the following formula [9-10]:

$$\Delta G^{inject} = E_{CB} - E_{OX}^{*} = E_{CB} - E_{OX} - E_{00} \qquad (13)$$

$$\Delta G^{reg} = E_{redox} - E_{OX} \qquad (14)$$

Here, E_{CB} refers to the TiO_2 CB lying at -4.0 eV, and E_{OX} and E_{OX}* represent the dye oxidation potential in its ground state and excited state, respectively, and E_{00} refers to the vertical transition energy. E_{redox} is the Fermi levels of electrolyte iodine/iodide. According to Koopman's theorem, E_{OX} can be calculated by taking negative of the dye HOMO.

$$\lambda_h = (E_0^+ - E_+) + (E_+^0 - E_0) \qquad (15)$$

$$\lambda_e = (E_0^- - E_-) + (E_-^0 - E_0) \qquad (16)$$

$$\lambda_{tot} = \lambda_h + \lambda_e \qquad (17)$$

Here, E_0, the neutral molecule's energy in the ground state; E_+/E_-, the energy of the cationic (anionic) optimized under the cationic (anionic) structure; *E+ 0/E- 0*, the cation (anion)'s energy with the geometry of the neutral molecule; *E0 +/E0 -*, the

neutral's energy with the geometry of the cationic (anionic) state [11].

The Newns-Anderson method was adopted to simulate the mixing of the lowest unoccupied molecular orbital (LUMO) on dye with the manifold virtue orbitals on TiO_2. The simulation was based on the shift in energy of the LUMO after grafting the TiO_2 surface and broadening width ($\hbar\Gamma$), which is defined by the Lorentzian distribution [12]:

$$L_{LUMO}(E)=\frac{1}{\left(E-E_{LUMO(ads)}\right)^2+\left(\frac{\hbar\Gamma}{2}\right)^2} \quad (18)$$

The broadening width $\hbar\Gamma$ is derived from the mean deviation of the LUMO (adsorbate) levels, which is evaluated as follows [13]:

$$\hbar\Gamma=\sum_i p_i\left|\varepsilon_i-E_{LUMO(ads)}\right| \quad (19)$$

$$\tau(fs)=\frac{658}{\hbar\Gamma} \quad (20)$$

where p_i and ε_i are the adsorbed portion of the ith molecular orbital and its corresponding orbital energy, respectively.

The above content has been added to the supporting documents.

Reference:

1. Tomás DM, Jesús BL, Rody SR, Daniel GM, Claudia D, Alessia C. Theoretical Study of the Effect of pi-Bridge on Optical and Electronic Properties of Carbazole-Based Sensitizers for DSSCs. *Molecules* **2020**, 25(16): 3670.
2. Zhang G, Musgrave CB. Comparison of DFT methods for molecular orbital eigenvalue calculations. *Journal of Physical Chemistry A* **2007**, 111(8): 1554-1561.
3. Singh M, Kanaparthi RK. Theoretical exploration of 1,3-Indanedione as electron acceptor-cum-anchoring group for designing sensitizers towards DSSC applications. *Solar Energy* **2022**, 273: 456-469.
4. Mandal S, Kandregula GR, Ramanujam K. Replacing aromatic pi-system with cycloalkyl in triphenylamine dyes to impact intramolecular charge transfer in dyes pertaining to dye-sensitized solar cells application. *Journal of Photochemistry and Photobiology A-Chemistry* **2020**,403: 112862.
5. DeSousa S, Lyu S, Ducasse L, Toupance T, Olivier C. Tuning visible-light absorption properties of Ru-diacetylide complexes: simple access to colorful efficient dyes for DSSCs. *Journal of Materials Chemistry A*, **2015**, 35: 18256-18264.
6. Stein T, Kronik L, Baer R. Reliable prediction of charge transfer excitations in molecular complexes using time-dependent density functional theory. *Journal of the American Chemical Society* **2009**, 13: 2818.

7. Senge MO, Fazekas M, Notaras EGA, Blau WJ, Zawadzka M, Locos OB, Mhuircheartaigh EMN. Nonlinear optical properties of porphyrins. *Advanced Materials* **2007**, 19: 2737-2774.
8. Patil DS, Avhad KC, Sekar N. Linear correlation between DSSC efficiency, intramolecular charge transfer characteristics, and NLO properties-DFT approach. *Computational and Theoretical Chemistry* **2018**, 1138: 75-83.
9. Li W, Wang J, Chen J, Bai FQ. Theoretical investigation and design of high-efficiency dithiafulvenyl-based sensitizers for dye-sensitized solar cells: the impacts of elongating π-spacers and rigidifying dithiophene. *Physical chemistry chemical physics* **2014**, 16(20): 9458-68.
10. Ashraful I, Hideki S, Hironori A. Molecular design of ruthenium(II) polypyridyl photosensitizers for efficient nanocrystalline TiO_2 solar cells. *Journal of Photochemistry & Photobiology, A: Chemistry* **2003**, 158(2): 131-138.
11.Wang HB, Zhao DP, Song P, Ma FC, Li YZ. Effect of charge transport channel and interaction of IDT type dyes on photoelectric characteristics. *Journal of Molecular Liquids* **2020**, 303: 112594.
12. Muscat JP, Newns DM. Chemisorption on metals. *Progress in Surface Science* **1978**, 9, 1.
13. El-Meligy AB, Koga N, Iuchi S, Yoshida K, Hirao K, Mangood AH, El-Nahas AM. DFT/TD-DFT Calculations of the Electronic and Optical Properties of Bis-N, N-Dimethylaniline-Based Dyes for Use in Dye-Sensitized Solar Cells. *Journal of Photochemistry & Photobiology, A: Chemistry* **2018**, 367: 332-346.

Table S1. The polarizability of the dye (a. u.).

Dye	α_{xx}	α_{xy}	α_{yy}	α_{xz}	α_{yz}	α_{zz}	α
TY6	1601	16	656	12	164	745	1001
CXC22	2614	-6	689	26	59	1154	1486
CHL7	1193	-98	1062	-128	-27	329	861

Table S2. Hyperpolarizabilities of three dyes (a.u).

Dye	β_{xxx}	β_{xyy}	β_{xzz}	β_{yyy}	β_{xxy}	β_{yzz}	β_{zzz}	β_{xxz}	β_{yyz}	B_{tot}
TY6	100684	1083	495	55	625	-470	-58	611	-122	101795
CXC22	204765	786	754	53	2415	-396	27	929	35	206449
CHL7	1207	3689	212	-2493	-505	-903	230	37	108	1419

Table S3. Excited states information of three co-sensitive configurations.

Dye	State	E(ev)	λ_{max}(nm)	f	CI (main)
H-H	S1	2.10	589.89	0.187	H-1→L+1 (0.63)
	S2	2.25	549.84	1.830	H→L (0.61)
	S3	2.45	505.76	0.035	H-2→L+1 (0.58)
	S4	2.71	456.32	0.052	H-2→L (0.50)
	S5	2.85	433.77	0.010	H-1→L (0.66)
	S6	3.13	395.66	0.003	H-2→L (0.64)
	S7	3.13	395.01	0.009	H→L+1 (0.57)
	S8	3.18	389.06	0.047	H-4→L (0.41)
	S9	3.32	372.49	0.730	H-1→L+3 (0.49)
	S10	3.36	368.57	0.156	H-4→L (0.37)
	S11	3.42	362.30	0.629	H-2→L+3 (0.52)
	S12	3.54	349.33	1.145	H-5→L (0.33)
H-T	S1	2.10	588.51	0.186	H-1→L+1 (0.63)
	S2	2.26	547.74	1.722	H→L (0.60)
	S3	2.45	505.56	0.041	H-2→L+1 (0.58)
	S4	2.71	456.97	0.066	H-2→L (0.50)
	S5	3.05	406.27	0.010	H-1→L (0.67)
	S6	3.19	387.64	0.027	H-4→L (0.41)
	S7	3.27	378.12	0.000	H→L+1 (0.61)
	S8	3.29	375.87	0.001	H-2→L (0.67)
	S9	3.34	370.81	0.746	H-1→L+3 (0.47)
	S10	3.35	369.41	0.382	H-4→L (0.34)
	S11	3.42	361.52	0.633	H-2→L+3 (0.53)
	S12	3.53	350.68	1.012	H-5→L (0.33)
S-S	S1	2.10	589.15	0.273	H-1→L+1 (0.63)
	S2	2.25	548.63	1.917	H→L (0.60)
	S3	2.45	504.59	0.040	H-3→L+1 (0.59)
	S4	2.71	456.04	0.104	H-2→L (0.50)
	S5	3.19	387.61	0.011	H-4→L (0.41)
	S6	3.34	370.95	0.055	H-4→L (0.35)
	S7	3.35	369.32	1.462	H-1→L+3 (0.57)
	S8	3.44	360.02	1.194	H-2→L+3 (0.57)
	S9	3.51	353.08	0.359	H-5→L (0.35)
	S10	3.69	335.19	0.287	H-7→L+1 (0.62)
	S11	3.75	330.28	0.000	H-1→L (0.70)
	S12	3.84	322.62	0.000	H→L+1 (0.69)

Table S4. The charge and hole contents are distributed in different parts of the three co-sensitive configurations (where D represents the CXC22 donor, P represents the CXC22 conjugate bridge, and A represents the CXC22 receptor).

Type	**State**	**D**	**P**	**A**	**CHL**	**D**	**P**	**A**	**CHL**
		Hole				Electron			
H-H	S1	0.11%	0.08%	0.05%	99.76%	0.01%	0.34%	0.20%	99.45%
	S2	11.83%	79.51%	8.49%	0.17%	1.72%	87.96%	9.80%	0.51%
	S3	0.05%	0.06%	0.07%	98.82%	0.01%	0.32%	0.18%	99.49%
	S4	42.83%	47.28%	7.83%	1.06%	1.97%	88.21%	9.42%	0.40%
	S5	0.14%	0.08%	0.04%	99.73%	0.35%	62.22%	36.85%	0.58%
H-T	S1	0.02%	0.01%	0.05%	99.91%	0.00%	0.04%	0.09%	99.87%
	S2	16.20%	75.75%	7.92%	0.13%	1.59%	85.09%	13.22%	0.10%
	S3	0.04%	0.04%	0.13%	99.80%	0.00%	0.06%	0.08%	99.86%
	S4	46.75%	45.82%	7.30%	0.13%	2.07%	90.03%	7.77%	0.13%
	S5	0.01%	0.01%	0.03%	99.96%	0.39%	66.77%	33.72%	0.13%
S-S	S1	0.00%	0.00%	0.00%	100.00%	0.00%	0.00%	0.01%	99.99%
	S2	11.97%	79.75%	8.28%	0.00%	1.71%	87.99%	10.29%	0.01%
	S3	0.00%	0.00%	0.00%	100.00%	0.00%	0.00%	0.01%	99.99%
	S4	45.95%	46.73%	7.31%	0.00%	2.09%	89.75%	8.16%	0.00%
	S5	25.12%	71.85%	3.03%	0.00%	2.86%	86.70%	10.43%	0.00%

Table S5. The amount of intermolecular charge transfer in the first five excited states of the three configurations (where D represents the CXC22 donor, P represents the CXC22 conjugate bridge, and A represents the CXC22 receptor).

Type	State	D	P	A	CHL	Net charge
H-H	S1	-0.00108	0.00265	0.00149	-0.00306	-0.00306
	S2	-0.10104	0.08447	0.01313	0.00344	0.00344
	S3	-0.00048	0.00259	0.00116	-0.00327	-0.00327
	S4	-0.41859	0.40930	0.01590	-0.00660	-0.00660
	S5	0.00217	0.62134	0.36802	-0.99153	-0.99153
H-T	S1	-0.00016	0.00030	0.00035	-0.00049	-0.00049
	S2	-0.14610	0.09342	0.05296	-0.00027	-0.00027
	S3	-0.00035	0.00022	-0.00047	0.00060	0.00060
	S4	-0.44680	0.44207	0.00472	0.0001	0.00001
	S5	0.00379	0.63760	0.35691	-0.99830	-0.99830
S-S	S1	0.00000	0.00004	0.00004	-0.00008	-0.0008
	S2	-0.10256	0.08243	0.02007	0.00006	0.0006
	S3	0.00000	0.00004	0.00003	-0.00006	-0.0006
	S4	-0.43868	0.43021	0.00843	0.0004	0.00004
	S5	-0.22256	0.14849	0.07402	0.00005	0.00005

Table S6. D/A Interfaces critical parameters (transition dipole moment (μ_{tr}), dipole moment difference ($\Delta\mu$), electronic coupling (V_{DA}), reorganization energy λ_{in} and λ (eV), Gibbs Free Energy change ΔG_{CR} (eV), Gibbs Free Energy charge in Charge separation ΔG_{CS} (eV), charge recombination rate K_{CR} (s^{-1}) and charge separation rate K_{CS} (s^{-1})).

μ_{tr}	$\Delta\mu$	V_{DA}	λ_{in}	λ	ΔG_{CR}	ΔG_{CS}	ΔK_{CR}	ΔK_{CS}
0.058	0.107	0.039	0.278	0.578	-2.07	-1.26	6.28	2.48×10^{8}

Figure captions:

Figure S1. The partial density of states of investigated dye/TiO_2 complexes.

Figure S2. The head-to-head (H-H), head-to-toe (H-T) and side-by-side type (S-S) configuration of the co-sensitization system.

Figure S3. Absorption spectra of three co-sensitive configurations.

Figure S4. CDD diagram of dye co-sensitized adsorption on TiO_2.

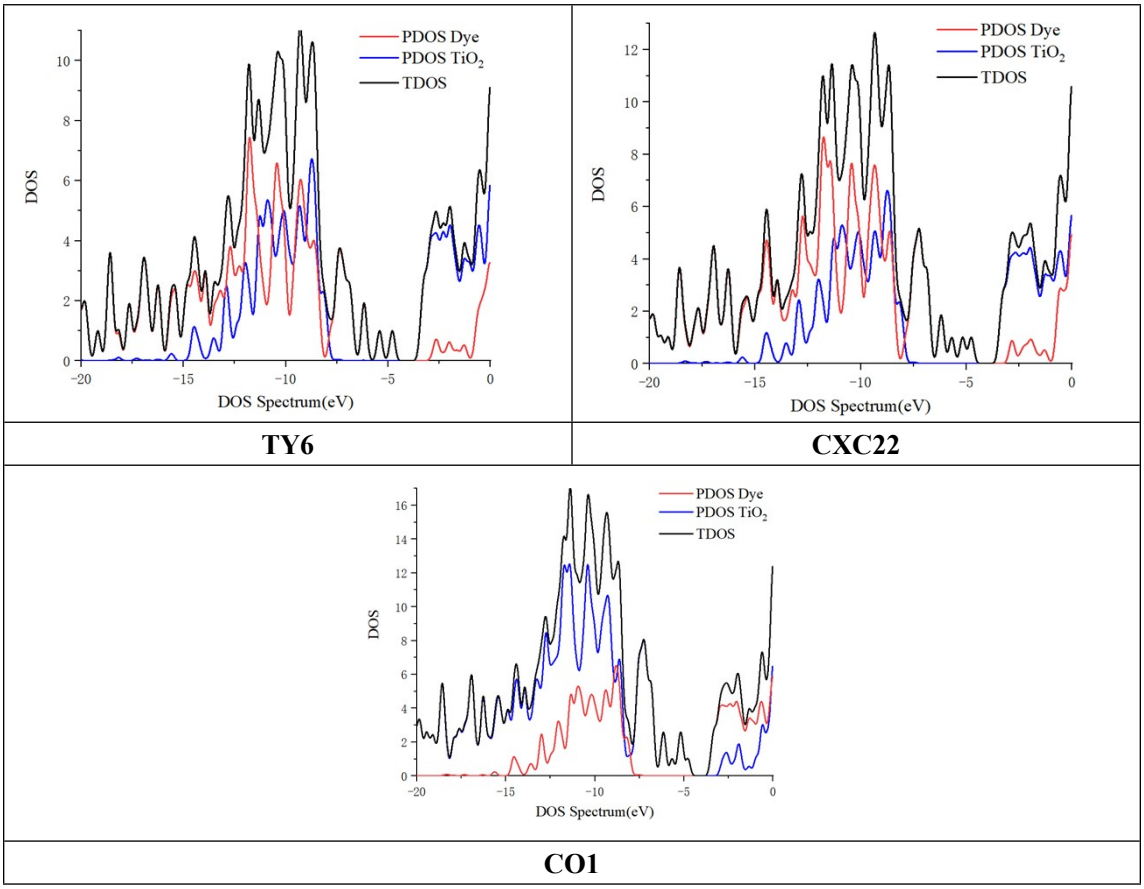

Figure S1. The partial density of states of investigated dye/TiO_2 complexes.

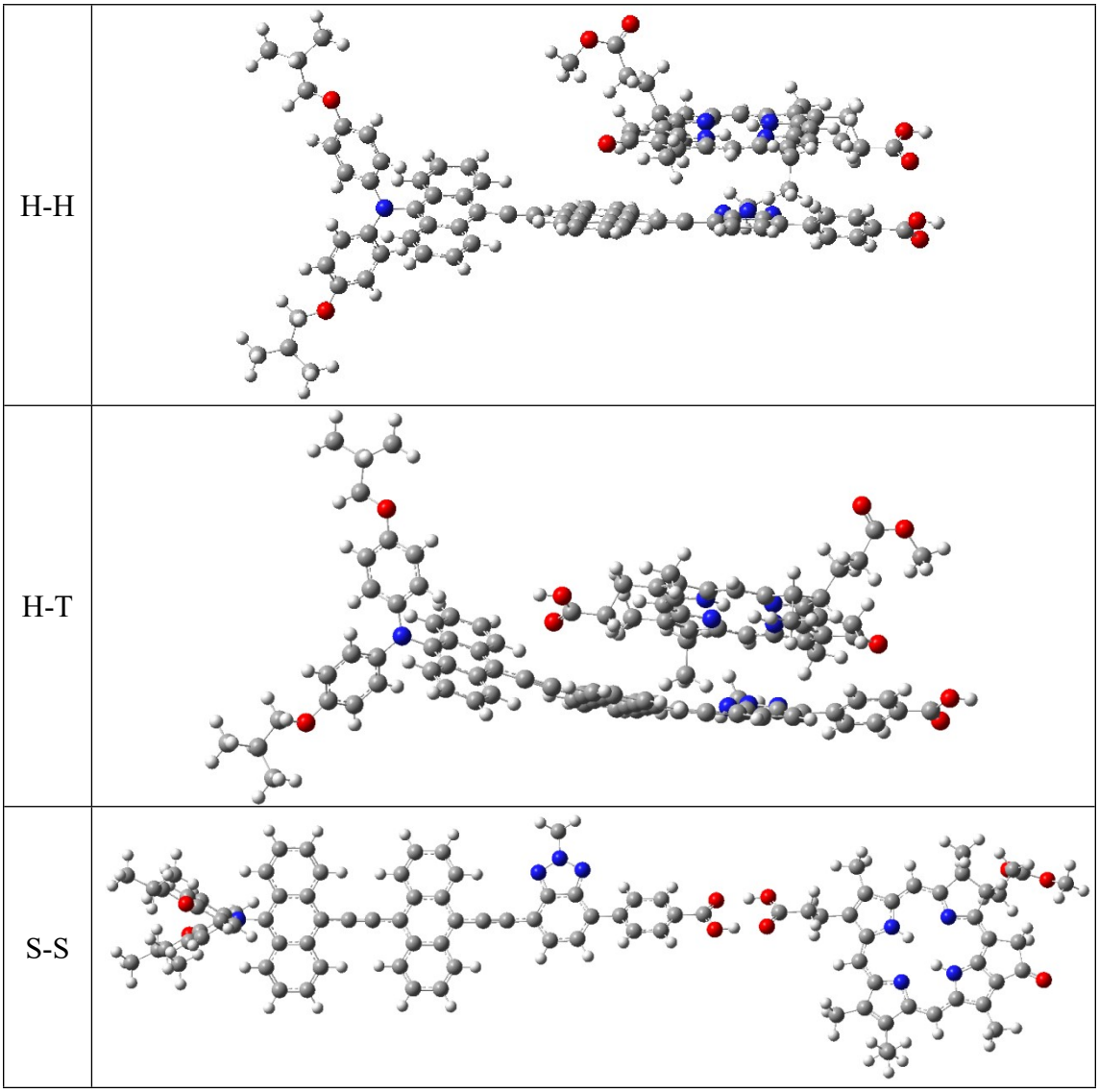

Figure S2. The head-to-head (H-H), head-to-toe (H-T) and side-by-side type (S-S) configuration of the co-sensitization system.

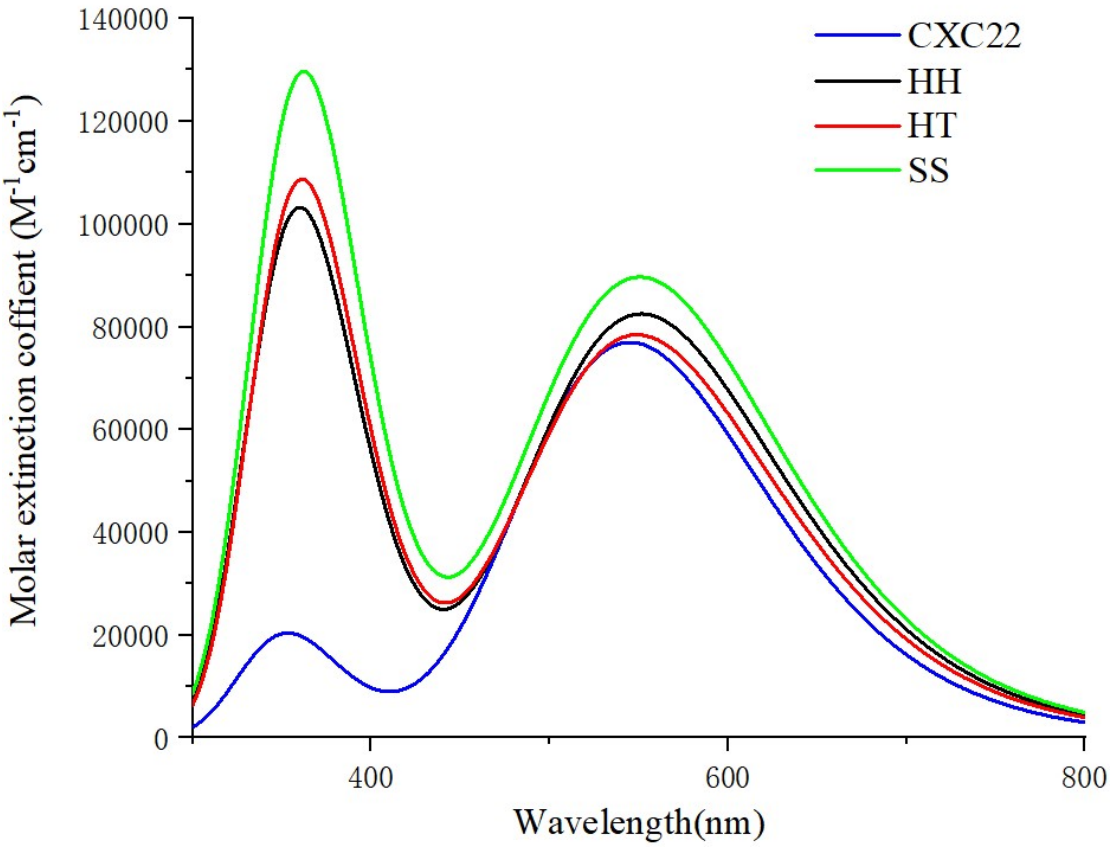

Figure S3. Absorption spectra of three co-sensitive configurations.

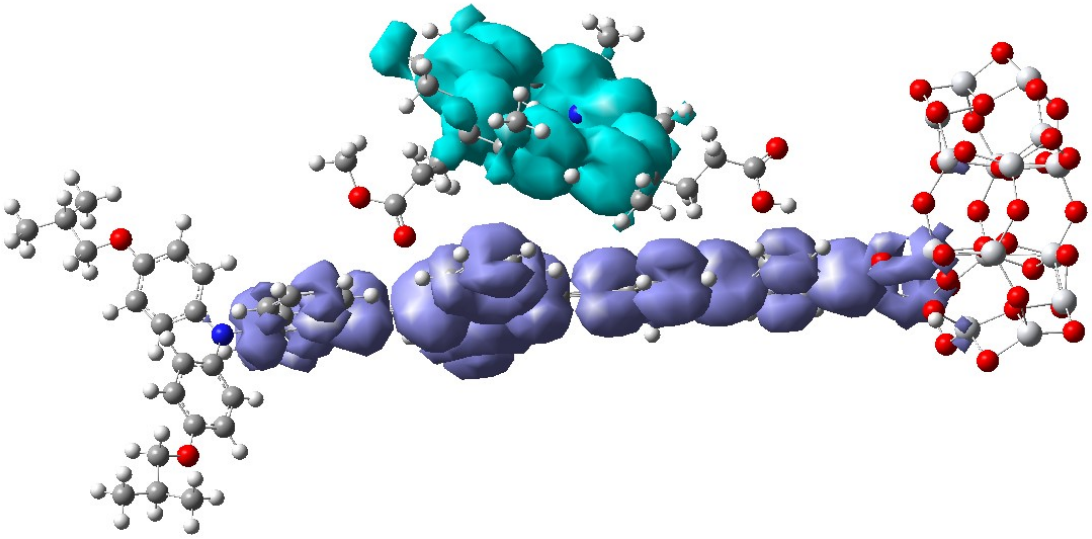

Figure S4. CDD diagram of dye co-sensitized adsorption on TiO_2.